Preprints.org

Article

Not peer-reviewed version

Enhancing Oil Recovery by Polymeric Flooding with Purple Yam and Cassava Nanoparticles

Hasanain A. Al-Jaber , Agus Arsad * , Muhammad Tahir * , Mustafa Jawad Nuhma , Sulalit Bandyopadhyay , Abdulmunem R. Abdulmunem , Anis Farhana Abdul Rahman , Zakiah binti Harun , Agi Augustine

Posted Date: 6 March 2023

doi: 10.20944/preprints202303.0087.v1

Keywords: enhanced oil recovery; polymer flooding; nano-polymer; cassava nanoparticles; purple yam nanoparticles

Preprints.org is a free multidiscipline platform providing preprint service that is dedicated to making early versions of research outputs permanently available and citable. Preprints posted at Preprints.org appear in Web of Science, Crossref, Google Scholar, Scilit, Europe PMC.

Copyright: This is an open access article distributed under the Creative Commons Attribution License which permits unrestricted use, distribution, and reproduction in any medium, provided the original work is properly cited.

Preprints (www.preprints.org) | NOT PEER-REVIEWED | Posted: 6 March 2023 doi:10.20944/preprints202303.0087.v1

Disclaimer/Publisher's Note: The statements, opinions, and data contained in all publications are solely those of the individual author(s) and contributor(s) and not of MDPI and/or the editor(s). MDPI and/or the editor(s) disclaim responsibility for any injury to people or property resulting from any ideas, methods, instructions, or products referred to in the content.

Article

Enhancing Oil Recovery by Polymeric Flooding with Purple Yam and Cassava Nanoparticles

Hasanain A. Al-Jaber [1,2], Agus Arsad [3,*], Muhammad Tahir [4,*], Mustafa Jawad Nuhma [5], Sulalit Bandyopadhyay [6], Abdulmunem R. Abdulmunem [7], Anis Farhana Abdul Rahman [8], Zakiah binti Harun [9] and Agi Augustine [10,11]

1 Institute for Oil and Gas, Faculty of Engineering, Universiti Teknologi Malaysia, 81310 UTM Skudai, Johor, Malaysia; hasanain1975@graduate.utm.my
2 Department of Chemical Industries Technologies, Southern Technical University, 61006 Zubair, Basrah, Iraq; hassanain.aljaber123.haj@gmail.com
3 UTM-MPRC Institute for Oil and Gas, Faculty of Engineering, Universiti Teknologi Malaysia, 81310 UTM Skudai, Johor, Malaysia; agus@utm.my
4 Chemical and Petroleum Engineering Department, United Arab Emirates University (UAEU), Al Ain P.O. Box 15551, United Arab Emirates; muhammad.tahir@uaeu.ac.ae
5 Chemical Engineering Department, College of Engineering, University of Al-Qadisiyah, Al-Diwaniyah City P.O. Box 88, Iraq; almuhandis_70@yahoo.com
6 Department of Chemical Engineering, Norwegian University of Science and Technology, Høgskoleringen 1, Trondheim 7491, Norway; sulalit.bandyopadhyay@ntnu.no
7 Electromechanical Engineering Department, University of Technology, Baghdad 10066, Iraq; 50192@uotechnology.edu.iq
8 School of Chemical and Energy Engineering, Faculty of Engineering, Universiti Teknologi Malaysia, Johor 81310, Malaysia; afarhana91@gmail.com
9 Institute for Oil and Gas, Faculty of Engineering, Universiti Teknologi Malaysia, 81310 UTM Skudai, Johor, Malaysia; zakiahharun22@gmail.com
10 Faculty of Chemical and Process Engineering Technology, College of Engineering Technology, Universiti Malaysia Pahang, 26300 Gambang, Pahang, Malaysia; aaagi2@live.utm.my
11 Centre for Research in Advanced Fluid and Processes (Fluid Centre), Universiti Malaysia Pahang, 26300 Gambang, Pahang, Malaysia; aaagi2@live.utm.my
* Correspondence: agus@utm.my (A.A); muhammad.tahir@uaeu.ac.ae (M.T); Tel.: +60195590545 (A.A); +971-509961678 (M.T.)

Abstract: Significant amount of oil remains in the reservoir after primary and secondary operations and to recover the remaining oil, enhanced oil recovery (EOR) can be applied as one of the feasible options remaining nowadays. In this study new nano polymeric materials have been prepared from purple yam and cassava starches. The yield of purple yam nanoparticles (PYNPs) was 85% and that of cassava nanoparticles (CSNPs) is 90.53%. Synthesized materials were characterized through particle size distribution (PSA), zeta potential distribution, Fourier transform infrared spectroscopy (FTIR), differential scanning calorimetry (DSC) and transmission electron microscopy (TEM). The performance of PYNPs in recovering oil was better than CSNPs as found from recovery experiments. Zeta potential distribution results confirmed the stability of PYNPs over CSNPs (-36.3 mV for PYNPs and -10.7 mV for CSNPs). The optimum concentration for these nanoparticles has been found from interfacial tension measurements and rheological properties and it was 0.60 wt.% for PYNPs and 0.80 wt.% for CSNPs. More incremental recovery (33.46%) has achieved for the polymer that contained PYNPs in comparison to the other nano-polymer (31.3%). This opens the inception for a new technology for polymer flooding that may replace the conventional method that depends on partially hydrolyzed polyacrylamide (HPAM).

Keywords: enhanced oil recovery; polymer flooding; nano-polymer; cassava nanoparticles; purple yam nanoparticles

© 2023 by the author(s). Distributed under a Creative Commons CC BY license.

Preprints (www.preprints.org) | NOT PEER-REVIEWED | Posted: 6 March 2023 doi:10.20944/preprints202303.0087.v1

1. Introduction

Due to the depletion of fossil resources and environmental challenges, biodegradable nanocrystals have received many attentions recent decades as new materials that can be involved in oil recovery [1]. These nanocrystal materials have gained outstanding properties in comparison to their counterparts, the microparticles, through their high surface to volume ratio as they are rigid materials at nano-meter scale [2–4]. Recent studies have shown that these nanomaterials can be used as fillers to improve the mechanical and barrier properties of bio-composites [5]. For these industrial applications a continuous endeavor is being taken into account to find the innovative solutions to achieve efficient and sustainable performance for these industries. Therefore, starch nanoparticles have been under focus through the high number of works that are devoted to develop the bio-composites by blending such starch nanoparticles into the biopolymeric matrices.

Starches, being biodegradable natural polymer are good candidate for the formation and production of nanoparticles. The market for starches is constantly growing, leading to a continuous search for products with specific features that meet industry requirements. The modification of starch with acid hydrolysis has been used to modify the structure of the granules and produce more soluble starch combinations [6]. Starch is usually hydrolyzed with mineral acids like acetic acid to remove the amorphous regions and retain the crystals [7,8].

Being used in oil recovery this is for sure one of the important applications of starch that has many challenges. Starch nanoparticles made from cassava and purple yam have received great interest because they are cheap, abundant, non-toxic and biodegradable materials [9,10]. During the processing of cassava and purple yam tubers into starch, the tuber is peeled off and then subjected to number of physical operations to extract starch and converted it into nano-size [11]. There are many factors that affect on the production of nanoparticles from starch. These factors include: process of hydrolysis, type of acid used, concentration of the acid, amylopectin to amylose ratio in starch, concentration of starch, time, temperature and speed of hydrolysis [12]. Also, ultrasound technique has been widely used to produce granules of nano-sized materials. On the contrary, exposure of polymer solution to high intensity of ultrasound radiation may reduce the molar mass for that starch.

Despite that water flooding can recover significant amount of oil, nonetheless this amount cannot exceed 50% from OOIP in the best scenario [13,14]. On the other side, common expectation from polymer flooding is only 15 to 20% incremental recovery over secondary flooding using synthetic polymers like HPAM [10]. Therefore, searching for natural polymer materials can help in reducing operational costs and in the same time may lead to improve in oil recovery. Nadia et al. [15] investigated the starch extracted from purple yam and evaluated its physicochemical and functional properties. For this purpose, five cultivars of yam were tested in their study. Scanning electron microscopy (SEM) was applied and three different kinds on granules based on size have been identified: round, oval and spherical. Furthermore, they measured the relative crystallinity of produced starch which is found between 20.6 to 30.4% with the second yam type.

Cassava starch-grafted polyacrylamide (CASPAM) hydrogel was synthesized according to a method proposed by Matovanni et al. [16] by using microwave technique and an initiator. The characterization of produced CASPAM was examined by FTIR and SEM analysis. To predict the behavior of the samples under reservoir conditions, the properties of CASPAM, such as water-solubility and viscosity were determined as a function for temperature, salt concentration and aging time. The FTIR spectra and SEM analysis for CASPAM confirmed that the polyacrylamide chains were successfully grafted onto the cassava starch radix. It was found that preparation of CASPAM with 10 g of acrylamide and 180 s of irradiation by using of a microwave has resulted in obtaining the highest grafting percentage and water solubility, which were 1565.53 and 96.06%, respectively. The results from this study showed that CASPAM combination helped in improving temperature resistance and durability to high salinity in relation to the observed reservoir conditions. This indicated that mixing cassava with polyacrylamide has good potential for oil recovery operations as an efficient, reliable and economic technology.

Based on previous researches, the current work aimed to synthesize starch nanoparticles from both cassava and purple yam and integrate them with constant concentration of HPAM (2000 ppm).

Preprints (www.preprints.org) | NOT PEER-REVIEWED | Posted: 6 March 2023 doi:10.20944/preprints202303.0087.v1

This achieved by involving each kind of starch nanoparticles in polymer flooding with HPAM and the new injection process has led to the improve of oil recovery. The optimum concentration for each kind of nano starch is estimated from interfacial tension measurements and rheological properties at temperature 60 °C. This temperature is chosen to simulate for the original temperature of Langgak oilfield in Sumatra, Indonesia. The experiments of polymer flooding are performed on a true crude oil brought from that oilfield and core samples similar in their properties to that of original field sandstone. The quality and property of synthesized nanoparticles for each kind are evaluated using PSA, TEM, Zeta potential distribution, FTIR and DSC analysis.

2. Materials and Methods

2.1. Materials

2.1.1. Buff Berea Core Samples

Five Buff Berea core samples are purchased from Atama Tech Sdn. Bhd., Skudai, Johor. Additional two cores are provided from reservoir laboratory – School of Chemical and Energy Engineering with properties similar to that of Buff Berea samples. These core samples are utilized in water and polymer flooding experiments. They have physical properties similar to that of original sandstone in the oilfield reservoir in Sumatra, Indonesia. Table 1 shows general properties for these core samples.

Table 1. Buff Berea core sample properties.

Product ID	SS-104
Formation	upper devonian
Permeability	150-350 mD KCL 400-500 mD N_2
Porosity	20-22%
UCS	3800-4500 psi
Homogeneous	YES
Perm by	KCL/N_2

2.1.2. Crude Oil

Crude oil with 31.9 °API was brought from Langgak oilfield in Sumatra, Indonesia. The viscosity of the crude oil is around 43.668 cp and in normal temperature (~ 25 °C) the oil phase structure is in solid state. Dealing with such oil needs special equipment in order to keep it in liquid state. To overcome this problem this oil has been treated with chemical solution called Fsol at a ratio (1:1). This chemical solution is purchased from innovative company called Innochems technologies Sdn. Bhd. located in Johor, Malaysia.

The said company did not reveal about the procedure used to manufacture Fsol but this solution has the ability to reduce the viscosity of oil and make it in liquid state at normal temperature without changing its main properties. This can be achieved through mixing the crude oil with this solution at the aforementioned ratio and then stirring the diluted oil for around 10 minutes using magnetic stirrer. In order to ensure the homogeneous composition for this oil after it mixed with Fsol, it was placed in oven at 60 °C for around 30 minutes before start using it for injecting.

2.1.3. Partially Hydrolyzed Polyacrylamide

Partially hydrolyzed polyacrylamide (HPAM) 0.5% aqueous solution brand R&M is purchased from Tricell Bioscience Resources Co. located in Taman Universiti, Johor, Malaysia.

Preprints (www.preprints.org) | NOT PEER-REVIEWED | Posted: 6 March 2023 doi:10.20944/preprints202303.0087.v1

2.1.4. Acetic Acid (CH_3COOH)

Glacial acetic acid (CH_3COOH) with purity of 99% was supplied by QREC (Asia) Sdn. Bhd. Selangor, Malaysia. All chemicals are commercially branded and they are used without further purification.

2.1.5. Purple Yam Tubers

18 kg of purple yam tubers were purchased from local market. It is known scientifically as "Dioscorea Alata" and other names are grater yam and water yam. It is one of various species of yam that were domesticated and cultivated within southeast Asia and New Guinea for their starchy tubers.

2.1.6. Native Cassava Starch

1 kg of native cassava starch was purchased from local market in Johor. Cassava is a versatile root vegetable that is widely consumed in several parts of the world, it is also what tapioca starch is made from. Cassava starch is a white powder made from tapioca that has been dehydrated and dried after being extracted.

2.2. Methods

2.2.1. Extraction of Purple Yam and Cassava Starch

18 kg tubers of purple yam were peeled, washed and crushed to fine particles using a grinder machine. Before begin the grinding process, small amount of water was added to the container of the grinding machine to ensure smooth cutting. The obtained thick solution from the grinding process was poured in large-size vessel through passing on 140 μm mesh size sieve from which it was left for precipitation to take effect after around 8 hours. The retained fibber on the sieve was washed with water so that more solution that contains starch can be retained on the vessel. After that, the collected starch was washed with pure water to remove any available fibber. Produced purple yam starch was dried in an oven at temperature 45 °C for about five hours to eliminate the moisture content and after then it was sun-dried for certain time to ensure complete drying. The sun-drying process is also useful for bleaching of starch and for reducing the cyanide content [17].

The dry weight of purple yam starch produced through this operation are obtained by using an electronic balance Shimadzu AY220. Produced starch was directed to pass through 72 μm mesh size (British standard) by using mechanical sieve to ensure that only small particle size of starch granules can be collected. The resulted fine starch was stored in an airtight container for analysis and further modifying to crystalline starch nanoparticles through acid hydrolysis that is assisted with ultrasonication. A sketch for this process is shown in Figure 1.

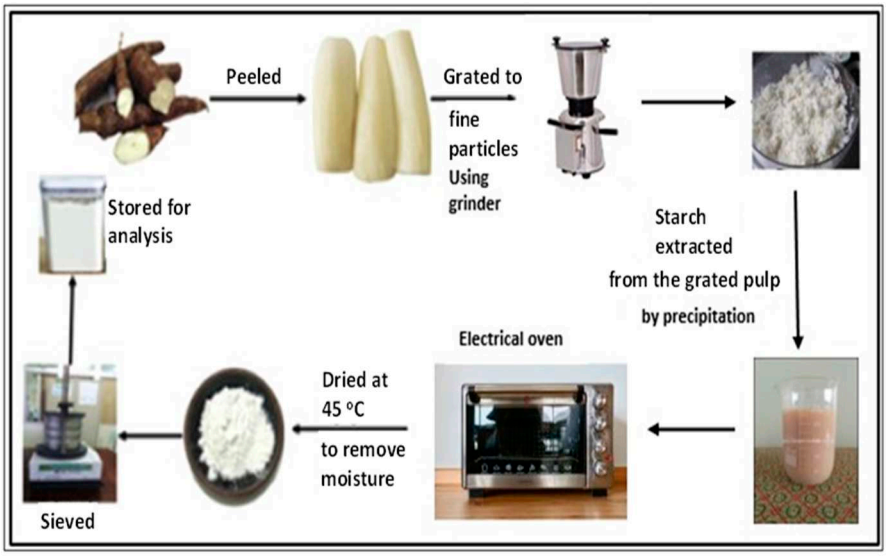

Preprints (www.preprints.org) | NOT PEER-REVIEWED | Posted: 6 March 2023 doi:10.20944/preprints202303.0087.v1

Figure 1. Purple yam starch preparation cycle from purple yam tubers.

2.2.2. Synthesis of Purple Yam and Cassava Nanoparticles

1 kg of native cassava starch was purchased from local market and it was ready to process to nano material. 40 g of purple yam and cassava starch are dissolved separately in 250 ml of acetic acid solution at concentration of 2.5 mol/l in an Erlenmeyer flask. Then, the resulting solution stirred continuously at a constant speed using a magnetic stirrer at temperature 45 °C for 5 days. After that, the solution was put in an ultrasonic instrument CREST LL TRANSONICS with frequency 40 kHz and power output 500 W for one hour. The use of ultrasonication with high intensity can help in reducing the molar mass of the solute and preventing nanoparticles aggregation [18].

The resulting solution was centrifuged for 20 minutes at a constant rate of 4000 rpm using ROTOFIX 32A instrument and the supernatant fluid was removed. The produced nanoparticles were washed twice in order to remove the remaining acetic acid. Produced nanoparticles were placed in an oven for 24 hours at 40 °C for drying process. Figure 2 represents aforementioned mechanism of production. Three independent parameters can affect on the production of nanoparticles: acid concentration (mol/l), temperature (°C) and time (days), whereas the output dependent responses are the yield (%) and particle size (nm) for produced nanoparticles. The accessibility range for these independent parameters was determined according to previous studies [18–20] as shown in Table 2.

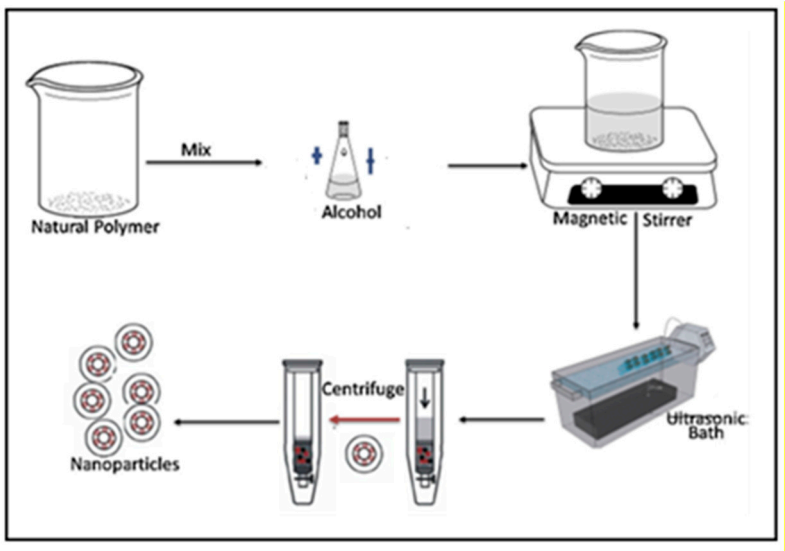

Figure 2. Synthesis process of starch nanoparticles from PYS and CAS.

Table 2. Independent variables and their limits for optimum production of nanoparticles.

Acid hydrolysis parameters (Independents variables)	Processability ranges	
	Minimum	Maximum
acid concentration, mol/l	2.2	3.6
temperature, °C	40	60
time, days	3	7

2.2.3. Particle Size Distribution (PSA)

The yield of produced nanoparticles from each kind can be calculated according to the following equation [21]:

$$\text{Yield } (\%) = W_{CSNP}/W_{NS} \times 100\% \quad (1)$$

where,

Preprints (www.preprints.org) | NOT PEER-REVIEWED | Posted: 6 March 2023 doi:10.20944/preprints202303.0087.v1

W_{CSNP} represents final weight of produced nanoparticles after the completion of drying process and W_{NS} is the initial weight of native starch for cassava and purple yam which is 40 g.

Particle size distribution gives important information about the size of particles and their geometrical shapes. This valuation was conducted in University Industry Research Laboratory (URIL UTM). Laboratory experiments for particle size are performed based on three major variables: intensity, volume and number percent for these nanoparticles.

2.2.4. Surface Charge for Nanoparticles

The stability of particles in a certain solution can be quantified by measuring Zeta potential for the particles. By using Electrophoretic light scattering, the velocity of the particles can be determined by measuring the frequency shift of the light scattered by the motion of particles. It was agreed that if the absolute zeta potential values are over 60 mV, then the particles are in excellent stability whereas if those values are above 30 mV, the particles accordingly are physically stable. Furthermore, if those values are lower than 5 mV this is an indication for the agglomeration of particles [21,22] as expressed in Table 3 [23].

Table 3. Stability behavior of colloids according to the value of Zeta potential.

Magnitude of Zeta potential (mV)	Stability behaviour
0 to 5	Rapid coagulation of flocculation
10 to 30	Incipient instability
30 to 40	Moderate stability
40 to 60	Good stability
> 61	Excellent stability

2.2.5. Polymer Rheology Analysis

It is important to characterize the polymer rheology to get a clear picture about it is suitability for the injection process. This has been done through the use of Brookfield RST rheometer from which the viscosity of the HPAM polymer, purple yam and cassava nanoparticles are measured and plotted versus the shear rate. These solutions are heated to the reservoir temperature 60 ^{o}C.

Approximately 68.5 ml of polymer solutions consisted from HPAM at concentration 5000 ppm and then HPAM (5000 ppm) with PYNPs and CSNPs are placed separately inside the cylindrical tube of the rheometer. The concentration of the purple yam/cassava nanoparticles varying from 0.25 to 1.25 wt.%. Number of measurements were obtained for a certain range of shear rate (300 – 1000 s^{-1}).

2.2.6. Optimum Concentration for Nanoparticles

In order to find the critical micelle concentration (CMC) for produced PYNPs and CSNPs, different concentrations (0.2, 0.4, 0.6, 0.8 and 1 wt.%) were prepaid by dissolving these particles in a brine solution (100 ppm). Then, 2000 ppm HPAM was added to the nanoparticle solution. The hybrid polymer from each kind was placed in contact with paraffin oil at 60 ^{o}C. Using a paraffin oil gives an acceptable approximation to the actual oil conditions in the reservoir oilfield [24]. The interfacial tension between the paraffin oil and hybrid polymers was calculated using KRUSS EasyDyne tensiometer (K20).

2.2.7. IFT Measurements

The interfacial tension (IFT) for different concentrations (0.2, 0.4, 0.6, 0.8 and 1 wt.%) for nanoparticles in the hybrid solution was measured in order to find the CMC which represents the optimum concentrations for PYNPs and CSNPs. The concentration of HPAM solution is held constant at 2000 ppm. The expected relation between IFT and concentration is that the IFT should decrease with increasing solution concentration until it reaches to a minimum value. The

Preprints (www.preprints.org) | NOT PEER-REVIEWED | Posted: 6 March 2023 doi:10.20944/preprints202303.0087.v1

corresponding value of concentration at this minimum value for IFT is the CMC for that nanoparticle solution.

2.2.8. Flooding Experiments

Flooding was initiated by inserting two hybrid polymers into the core flooding instrument. The first nano-polymer is consisted of 2000 ppm HPAM plus 0.60 wt.% PYNPs. The second polymer solution is consisted of 2000 ppm HPAM and 0.80 wt.% CSNPs. Three Buff Berea core samples have placed inside the saturation vessel and allowed to be vacuumed. Then, the vessel is connected to a vacuum pump for three hours to withdraw the air from inside the core samples. Brine was prepared at 100 ppm by dissolving 10 g of NaCl in 1000 ml volume of distilled water. Brine was carefully injected inside the saturation vessel by means of the same vacuum pump.

When the brine solution fully filled the free space inside the saturation vessel, the excess brine began to discharge out from the vessel and collect inside a conical flask. Then, the vacuum pump is turned off and the saturation vessel is connected to a Teledyne pump. The pressure inside the vessel is increased gradually through the injection of 10 cm3/min brine through the Teledyne pump. When the pressure inside the saturation vessel reached around 2000 psi, the brine injection from the accumulator was stopped. The vessel remained under this pressure for two to three days in order to fully saturate the core samples with the brine.

After the cores are completely saturated with brine, they are ready to be saturated with the crude oil. The brine is removed from the accumulator and the saturation vessel was opened and two core samples were removed and placed in a 1000 ml beaker containing brine to keep their saturation. After that, the remaining core sample was inserted into the confining vessel and the crude oil that was previously mixed with Fsol is injected. Nitrogen gas was pumped into the confining vessel to assist in spreading the oil inside the sandstone pores. Teledyne pump was operated at volumetric flow rate 8 cm3 per minute to inject the oil inside the confining vessel. The output from injection is settled in a 50 ml cylinder. After the oil saturate the core sample it began to push on the water (brine) from inside the core allowing it to exit and accumulate in the cylinder. This process is continued until excess oil (just few drops) was discharged out [25]. At this point the oil injection process is stopped and the volume of water produced during the oil injection is equal to the original oil in place (OOIP). The basic principle behind this fact is related to the law of conservation of mass.

After knowing the quantity of original oil in place (OOIP), the volume of water still inside sandstone core after oil injection/saturation can be estimated. This is the irreversible water content that cannot be retained after oil injection. Therefore, the initial oil saturation is always less than 100% under these conditions. After the saturation of the core sample with crude oil, water flooding is initiated by injection 5 cm^3/minute brine into the core sample. The output from water flooding is accumulated in the 50 ml cylinder and its quantity is estimated every 3 minutes. The water flooding is then resumed until one pore volume (1 PV) of water was injected [26].

The polymer flooding is initiated after water flooding and it is related with the injection of the two aforementioned HPAM-nano polymers. 3 to 3.5 cm^3/minute of nano polymer is injected and the output to the collecting cylinder is checked every three minutes as in water flooding. In order to maintain the temperature for water and polymer flooding around 60 ^oC, the confining vessel was placed inside an electrical oven after setting its temperature to 60 ^oC. The temperature inside the oven is verified to be around 60 ^oC by measuring the temperature through a thermocouple. The polymer flooding is continued until 2 PV [27] of nano-polymer was injected inside the core sample. The oil recovery percent for the recovery process (RF) can be calculated from the following equation [28]:

$$RF = (\text{volume of oil produced at cylinder} / OOIP) * 100\% \quad (2)$$

Preprints (www.preprints.org) | NOT PEER-REVIEWED | Posted: 6 March 2023 doi:10.20944/preprints202303.0087.v1

3. Results and Discussion

3.1. TEM Analysis

The final weight of produced nanoparticles was found to be 36.21 g for CSNPs and 34 g for PYNPs. Based on that, the yield of produced nanoparticles for CAS and PYS are 90.53 and 85%, respectively. Figures 3 and 4 show particle size distribution and TEM analysis result for sample of PYNPs and CSNPs, respectively. Figures 5 and 6 show the TEM images for PYNPs and CSNPs with some morphological details. These images demonstrate that the particles are well distributed with particle size ranging from 5.4 to 13.8 nm for PYNPs (Figure 5a) and 12.2 to 24 nm for CSNPs (Figure 6a). Large quantity of small particle size for PYNPs and CSNPs were produced during the preparation process for these nanoparticle components [29].

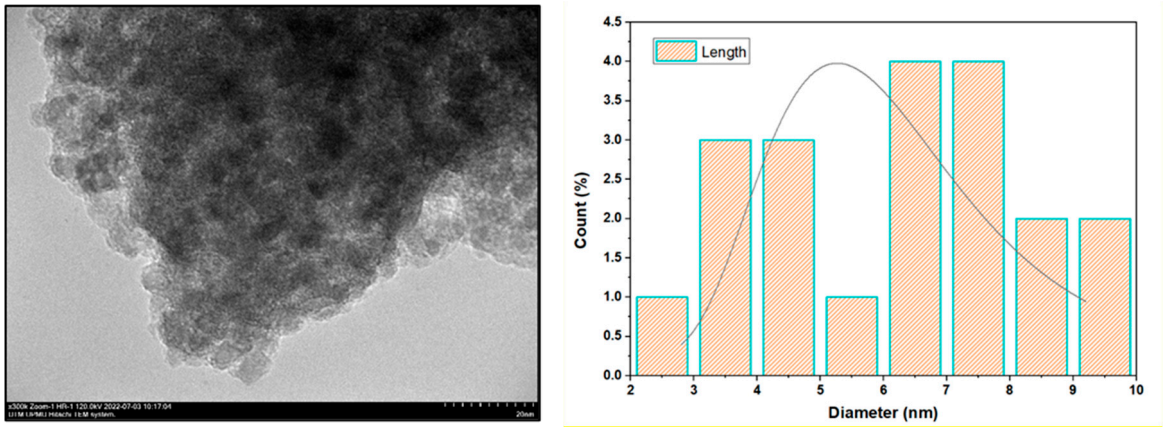

(**a**) (**b**)

Figure 3. Sample of PYNPs: (a) TEM spectra; (b) Particle size distribution.

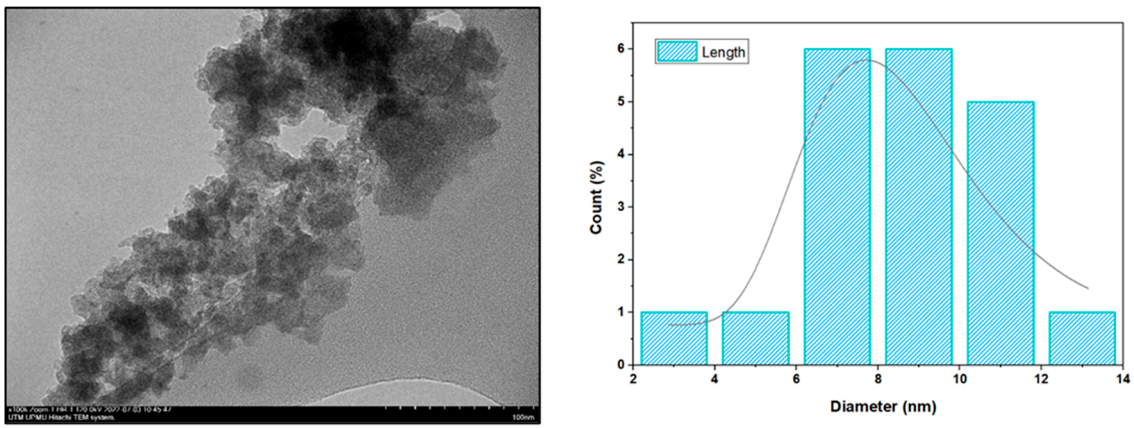

(**a**) (**b**)

Figure 4. Sample of CSNPs: (a) TEM spectra; (b) Particle size distribution.

Preprints (www.preprints.org) | NOT PEER-REVIEWED | Posted: 6 March 2023 doi:10.20944/preprints202303.0087.v1

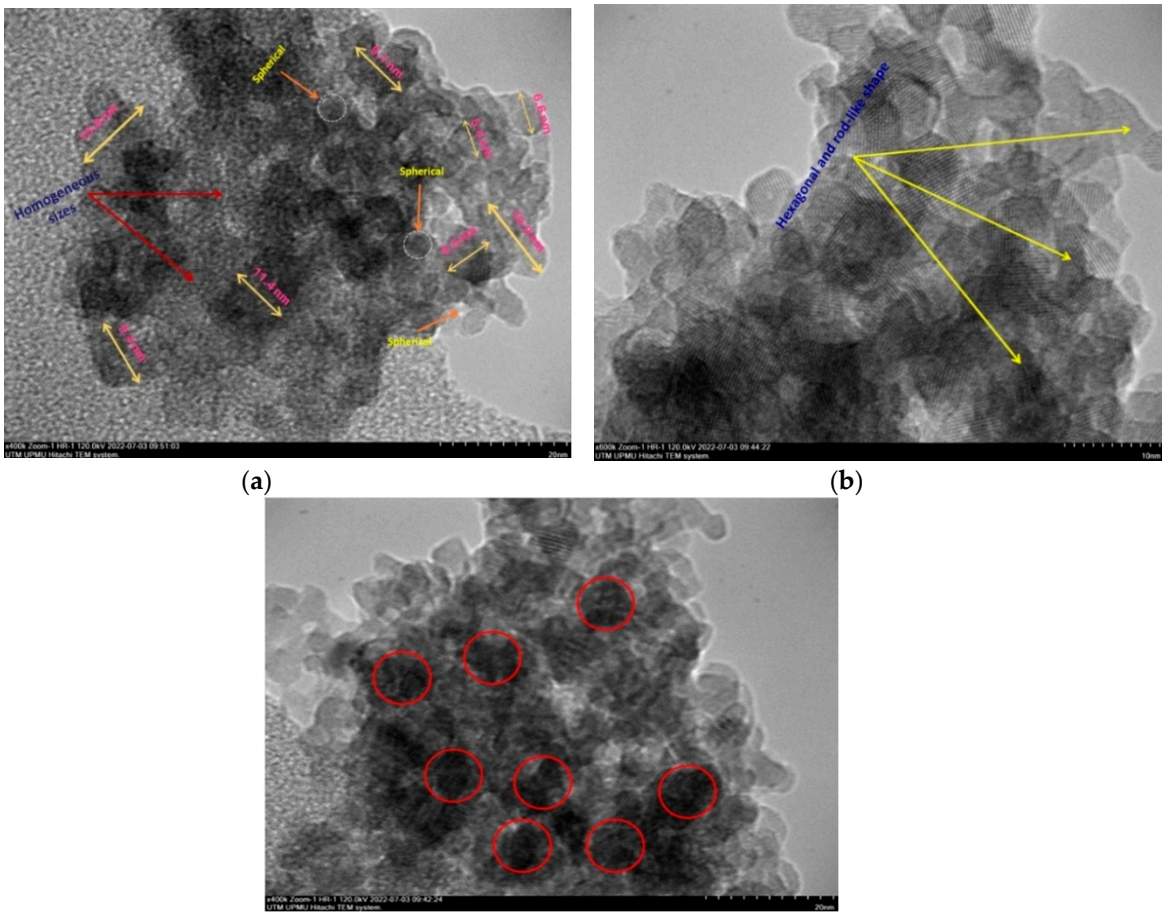

(a) (b)

(c)

Figure 5. TEM images for PYNPs: (a) homogenous size particles; (b) hexagonal and rod-like shape; (c) nucleation due to cavitation bubbles.

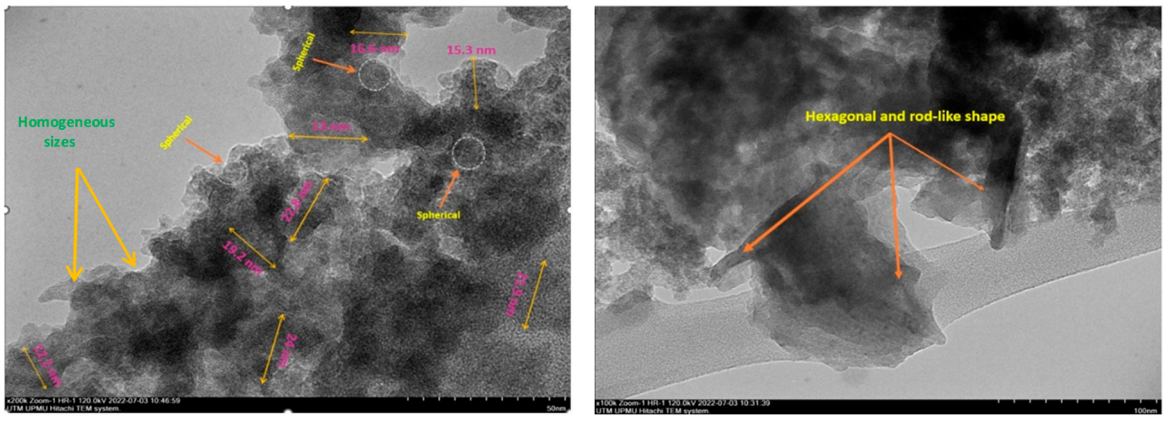

(a) (b)

Preprints (www.preprints.org) | NOT PEER-REVIEWED | Posted: 6 March 2023 doi:10.20944/preprints202303.0087.v1

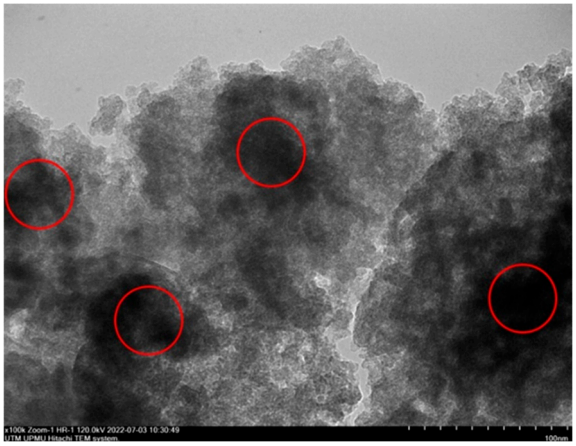

(c)

Figure 6. TEM images for CSNPs: (a) homogenous size particles; (b) hexagonal and rod-like shape; (c) nucleation due to cavitation bubbles.

The average particle size for PYNPs and CSNPs based on intensity percent (which is useful in detecting small amounts of aggregation) was 363.12 and 52.92 nm, respectively. The shape of produced nanoparticles varied from spherical, hexagonal and rod-like, which it is shown in TEM images. As Ku and Maynard [30] stated, the combination of monopolar electric forces for these nanoparticles which is controlled by applied temperature have well contributed to the formation of large portion of non-agglomerated and spherical nanoparticles.

As the coagulation between particles decrease rapidly due to quenching and dilution effects [31], the particles move from spherical shape to other forms such as hexagonal and rod-like as shown in Figures 5 and 6. Free radicals were produced during cavitation process, which involves the formation, growths and collapse of bubbles between the particles [32]. The violent collapse of these cavitation bubbles is illustrated by red circles in Figures 5 c and 6 c.

The morphology and surface appearance of the nanoparticles for both kinds were detected by TEM analysis. The micrographs reveal that both purple yam NPs (Figure 5a) and cassava NPs (Figure 6a) are approximately hexagonal in shape with fairly smooth surfaces and monodispersed with uniform size. As it was mentioned before, the size of the PYNPs (363.12 nm) is bigger than CSNPs (52.92 nm). The polydispersity index (PDI) which its numerical value ranges from 0 for a perfectly uniform sample regarding particle size to 1 for a highly polydisperse sample with multiple particle size populations [33,34] is an important factor that contribute to the stability and homogeneous distribution for the produced nanoparticles. Its mean value was calculated for PYNPs as 0.937 and that for CSNPs as 0.916 based on intensity percent analysis. Table 4 displays the hydrodynamic particle size, polydispersity index (PDI) and zeta potential for PYNPs and CSNPs in the aqueous solution.

Table 4. Properties of produced nanoparticles.

NPs type	Mean particle size (nm)	Mean PDI	Mean zeta potential (mv)	Stability status
PYNPs	363.12	0.937	-36.3	Moderate (More stable particles)
CASNPs	52.92	0.916	-10.7	Incipient (Less stable particles)

3.2. Zeta Potential Outputs

Three runs have been processed for zeta potential analysis for PYNPs and CSNPs as illustrated in Figures 7 and 8, respectively. The mean zeta potential for PYNPs was -43.9, -33.8 and -31.3 mV for the green, yellow and red curves, respectively. This indicates that the stability of the particles is high enough that the nanoparticles did not aggregate [35,36]. This makes PYNPs suitable candidate for injection in the oilfield reservoirs. On the other hand, the mean zeta potential for CSNPs obtained

Preprints (www.preprints.org) | NOT PEER-REVIEWED | Posted: 6 March 2023 doi:10.20944/preprints202303.0087.v1

from the same instrument was -9.3, -10.3 and -12.4 mV for the same color combination (green, yellow and red) as shown in Figure 8. This means that CSNPs are critically stable in water formation.

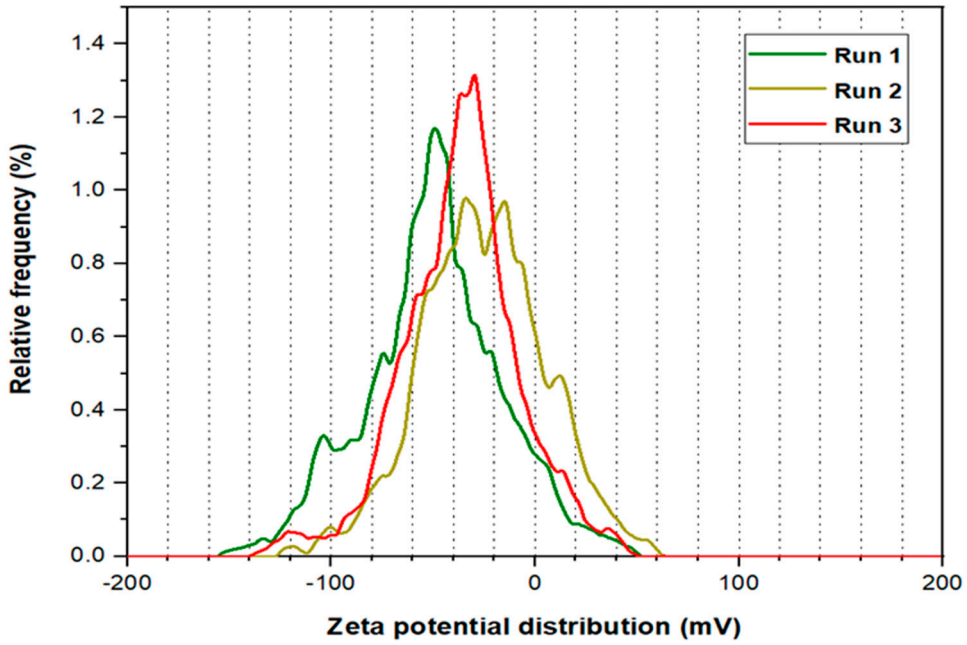

Figure 7. Zeta potential distribution for PYNPs.

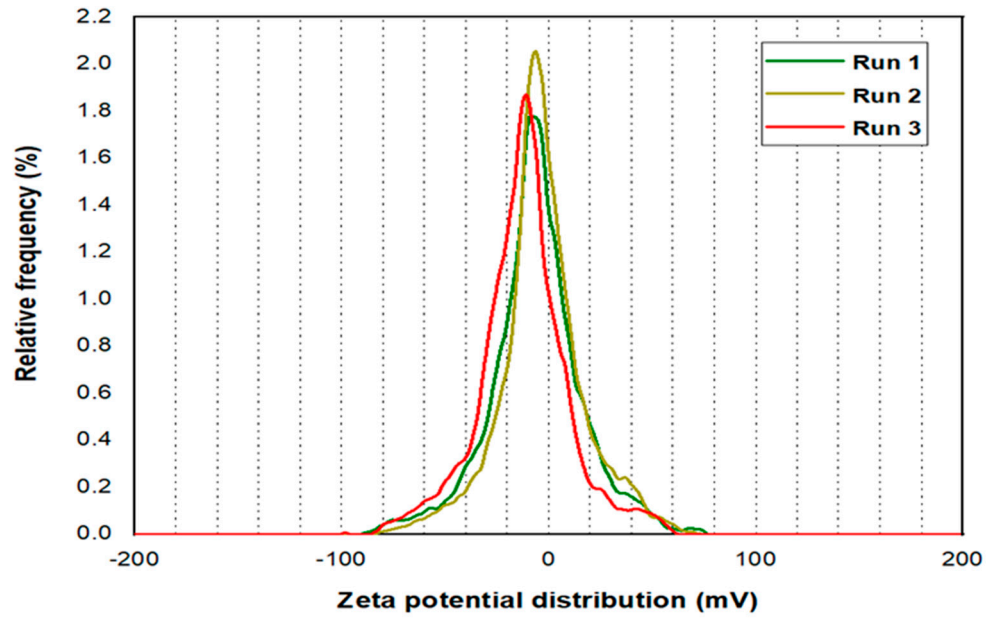

Figure 8. Zeta potential distribution for CSNPs.

3.3. FTIR Formation Analysis

FTIR spectra for both PYNPs and CSNPs is shown in Figure 9. For CSNPs the results for FTIR analysis can be explained as follow: peak value of 3371 cm^{-1} represents a medium N-H stretching bond consist mainly of aliphatic primary amines [37]. The peak of 2933 cm^{-1} refers to medium C-H stretching and indicates that the main compound within this absorption is consisted of alkanes. The peak value of 2345 cm^{-1} indicates a strong O=C=O stretching bond and it is consisted mainly of carbon dioxide. The peak of 1648 cm^{-1} represents a strong C=O stretching bond with materials composed of

Preprints (www.preprints.org) | NOT PEER-REVIEWED | Posted: 6 March 2023 doi:10.20944/preprints202303.0087.v1

component lactam. Lactam (which is the combination of the words lactone + amide) is a cyclic amide and it is derived essentially from an amino alkanoic acid [38].

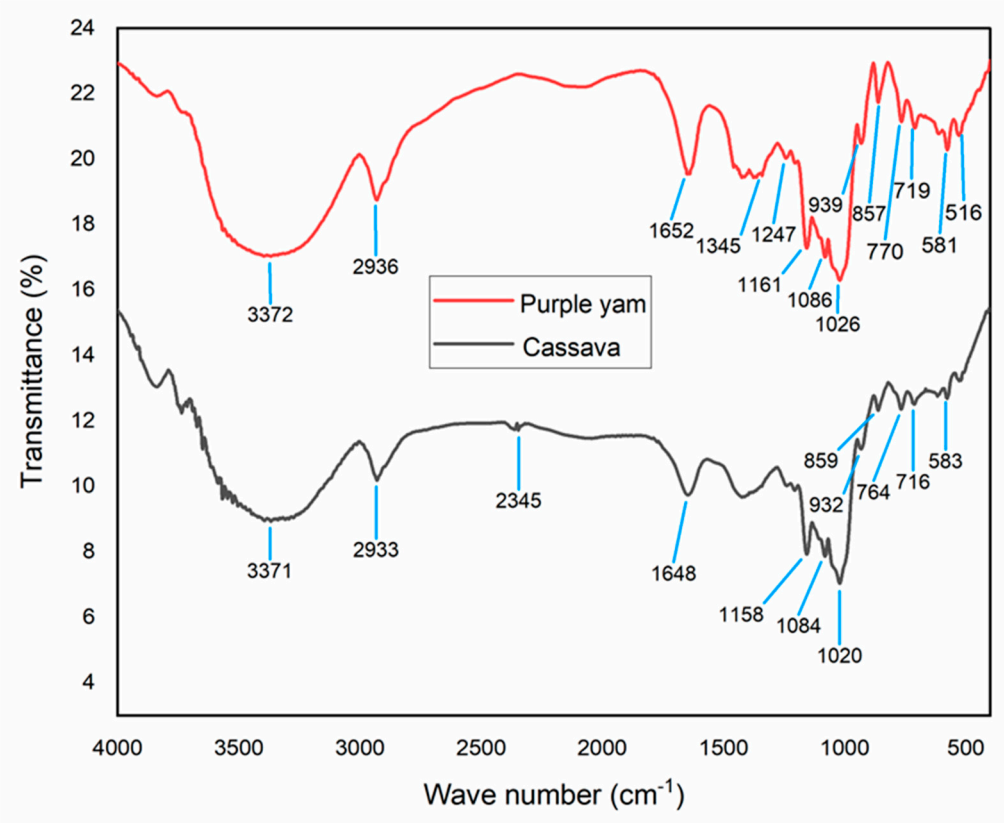

Figure 9. Relation between transmittance and wave number for PYNPs and CSNPs.

The value of 1158 cm^{-1} refers to a strong C=O stretching and the main compound for this combination is consisted of tertiary alcohol. The value of 1084 cm^{-1} represents also a strong C=O stretching bond and consisted mainly of primary alcohol. The peak value of 1020 cm^{-1} refers to a strong and broad CO-O-CO stretching bond and consisted of anhydride. The peak value of 932 cm^{-1} explains a strong C=C bending bond consisted from alkene compound that is trans disubstituted [39]. The peak value of 859 cm^{-1} explains a strong C-Cl stretching bond and it is made up of halo compounds. The peak of 764 cm^{-1} refers to medium C=C bending bond that consisted of alkenes in tri-substituted form. The peak value of 716 cm^{-1} refers to a strong C=C bending also made up of alkenes but in cis-disubstituted position [40,41]. The last peak value of 583 cm^{-1} for cassava nanoparticles represents a strong C-I stretching bond that is consisted of halo compounds.

The analysis for PYNPs can be interpretated as follows: the peak value of 3372 cm^{-1} represents a medium N-H stretching bond consist of aliphatic primary amines. The value of 2936 cm^{-1} refers to medium C-H stretching bond and indicates that main compound is alkane. The peak of 1652 cm^{-1} represents a strong C=O stretching bond composed of lactam. The peak value of 1345 cm^{-1} refers to a medium O-H bending bond that is consisted of alcohol. The peak value of 1247 cm^{-1} indicates a strong C-O stretching bond that includes alkyl-aryl-ether compound [42,43]. The value of 1161 cm^{-1} refers to a strong C-O stretching that is consisted of tertiary alcohol. The peak of 1086 cm-1 refers to a strong C-O stretching that is consisted of aliphatic ether. The peak of 1026 cm^{-1} refers to a strong S=O stretching bond that is consisted of sulfoxide. The peak value of 939 cm^{-1} is related to a strong C=C bending bond that belongs to alkene compounds in the trans disubstituted. The value of 857 cm^{-1} is related to a strong C-Cl stretching bond which is related to halo compound. The peak value of 770 cm^{-1} do not refers to any compound and this is possible because of the fact that not all frequencies refer to a related compound [44]. Same thing applies to the peak value of 719 cm^{-1}. The peak of 581 cm^{-1} refers to a strong C-I stretching bond that belongs to halo compound. And finally, the peak value of 516 cm^{-1} refers to a strong C-Br stretching bond that belongs to a halo compound [45].

Preprints (www.preprints.org) | NOT PEER-REVIEWED | Posted: 6 March 2023 doi:10.20944/preprints202303.0087.v1

3.4. DSC Thermogram

The basic characteristics that can been seen from Figure 10 can be summarized in the following points:

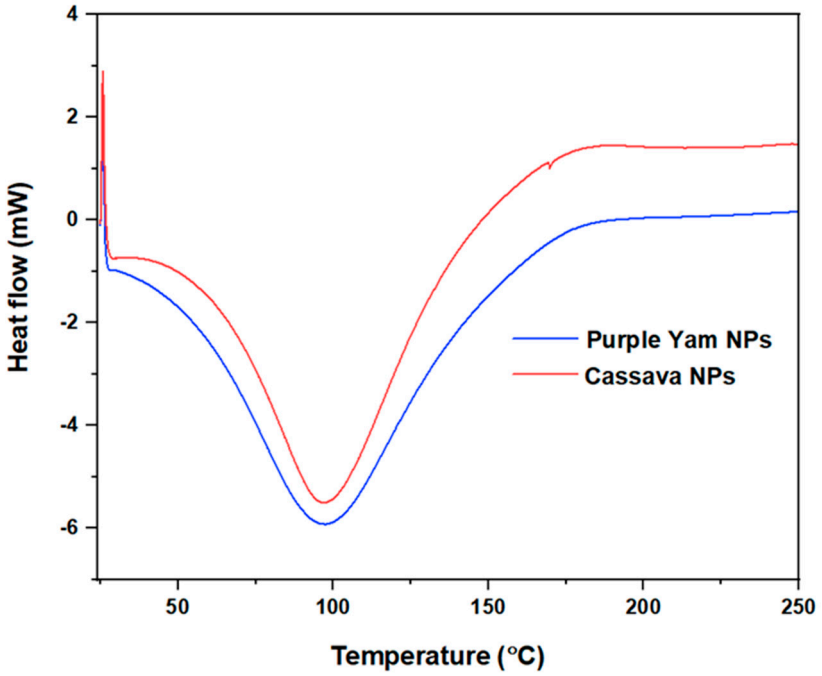

Figure 10. DSC thermograph for PYNPs and CSNPs.

1. The glass transition region is not clear and continuous as it seen from the upper left side of the curve and this give an impression that these nano polymers are more likely to have well-recognized crystalline regions during the heating process comparison to the amorphous region.

2. Due to the sensitivity of the nano polymers that are made from starch extracted from purple yam and cassava, the crystallinity regions can interfere with the melting regions. For this reason, there is no distinguished region specialized for the melting part, therefore, the crystallinity temperature can be considered the same as the melting temperature which is 97.6 °C for PYNPs and 97.8 °C CSNPs as seen from the curve.

3. There are high similarities between the components and structures of PYNPs and CSNPs in such a way that the DSC thermograph for them is similar. CSNPs curve is somehow higher than that of PYNPs. For this sense the melting temperature is nearly the same for each other (difference of 0.2 °C). From another aspect, choosing PYNPs for polymer flooding for the first time to improve oil recovery is not something far from logic as CSNPs itself has been already tested in polymer flooding and good results for oil recovery have been obtained [17,18].

3.5. Rheological Properties of PYNPs and CSNPs

The polymer rheology for HPAM with PYNPs and CSNPs is shown in Figures 11 and 12, respectively. From these figures, the viscosity increased with increasing shear rate for both PYNPs and CSNPs. At concentration of 1.25 wt.% PYNPs the viscosity of the solution is the highest whereas at concentration 0.25 wt.% the measured viscosity was the lowest until shear rate value of 500 s^{-1}. After this value, the lower viscosity was observed for the solution that contains 1 wt.% PYNPs. This indicates that concentration of 1.0 wt.% PYNPs at higher values of shear rate is considered as the best concentration that leads to a lower viscosity.

Preprints (www.preprints.org) | NOT PEER-REVIEWED | Posted: 6 March 2023 doi:10.20944/preprints202303.0087.v1

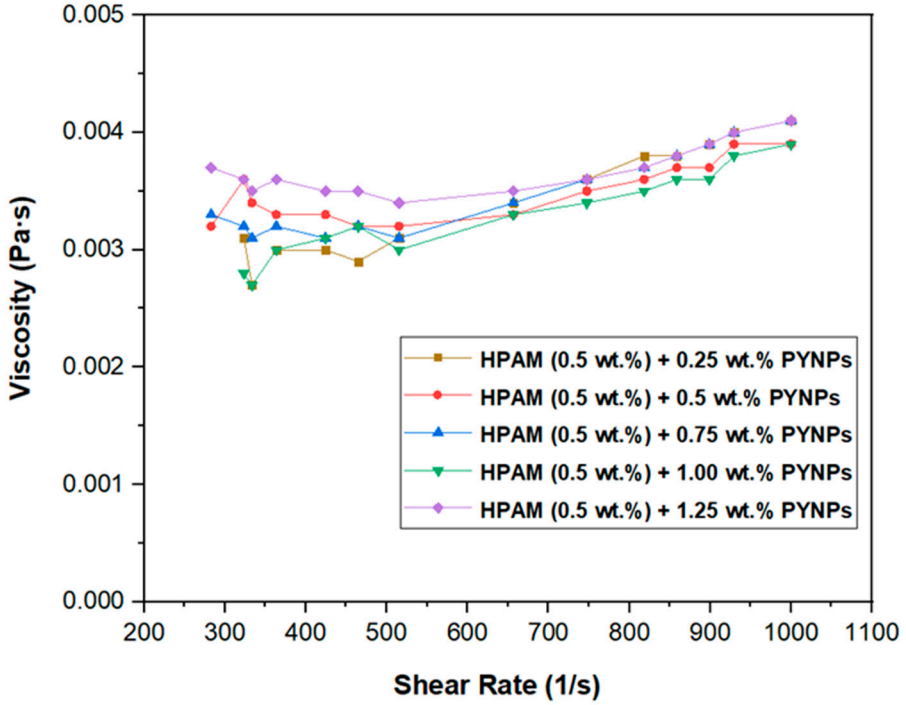

Figure 11. Relation between viscosity and shear rate for HPAM solution with five concentrations of PYNPs at 60 °C.

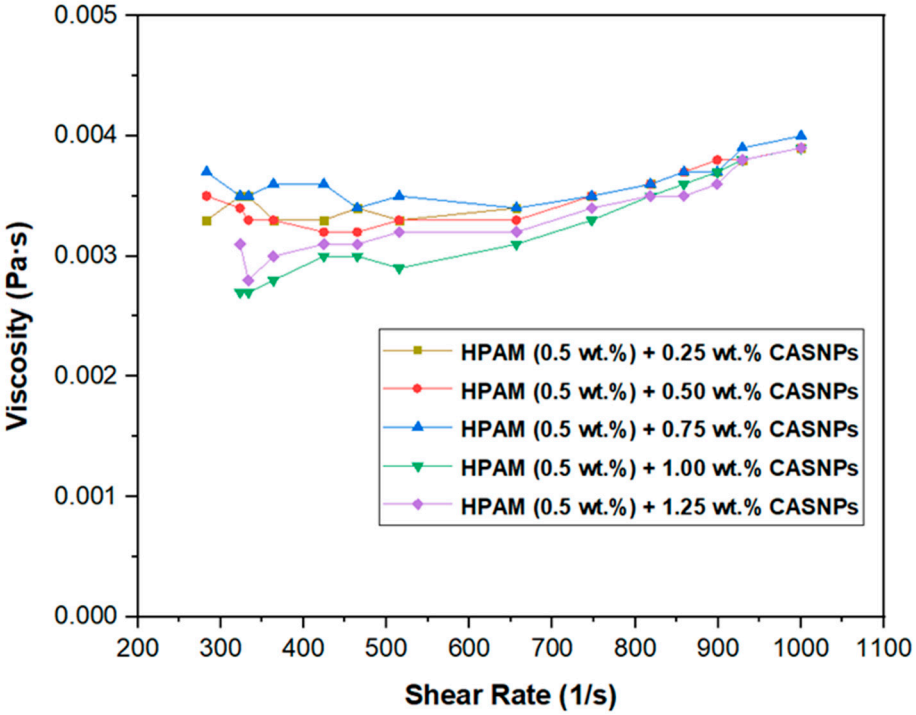

Figure 12. Relation between viscosity and shear rate for HPAM solution with five concentrations of CSNPs at 60 °C.

The variation of viscosity for HPAM with CSNPs looks more irregular in comparison with the previous solution especially at higher shear rates (more than 750 s^{-1}). For this solution, it was found from the resulting curve that the concentration of 0.75 wt.% for CSNPs gives higher viscosity for shear rate values from 300 to 1000 s^{-1}, whereas 1 wt.% CSNPs solution gives the lower viscosity rates for

Preprints (www.preprints.org) | NOT PEER-REVIEWED | Posted: 6 March 2023 doi:10.20944/preprints202303.0087.v1

shear rate values ranging from 300 to 850 s^{-1}. After exceeding shear rate value of 850 s^{-1}, the solution of 1.25 wt.% CSNPs becomes the one that gives lower viscosity in comparison to the concentrations. Therefore, for this variation the practical concentration for cassava nanoparticle solution with HPAM (0.5 wt.%) should be something between 0.75 and 1.25 wt.%. The presence of PYNPs and CSNPs has improved the polymer rheology of HPAM solution to a certain degree.

The inclusion of NPs has improved the viscosity and viscoelastic properties of HPAM solution [46]. NPs/HPAM hybrid solution showed a thermal stability at T= 60 ºC which is the temperature of the Indonesian oil reservoir. The rheology test also indicated that seeding PYNPs and CSNPs has facilitated the cross links among polymer molecules and made the hybrids more elastically dominant.

3.6. Effect of IFT on PYNPs and CSNPs Concentration

IFT at temperature 60 ºC for PYNPs and CSNPs with HPAM are shown in Figures 13 and 14, respectively. As seen from these figures, the IFT decreases with increasing concentration of nanoparticles in the hybrid polymer until it reaches to a minimum value at a certain (critical) concentration from which increasing further the concentration of the nanoparticles in the hybrid polymer has led to an increase of IFT value [47]. This 'critical' value is 0.62 wt.% for PYNPs and 0.80 wt.% for CSNPs in the polymer solution.

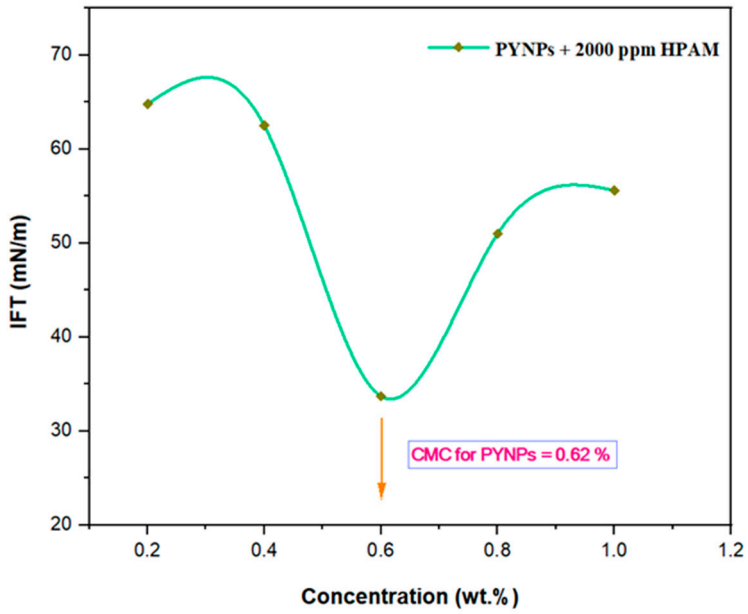

Figure 13. Relation between IFT and concentration for HPAM/PYNPs solution at 60 ºC.

Preprints (www.preprints.org) | NOT PEER-REVIEWED | Posted: 6 March 2023 doi:10.20944/preprints202303.0087.v1

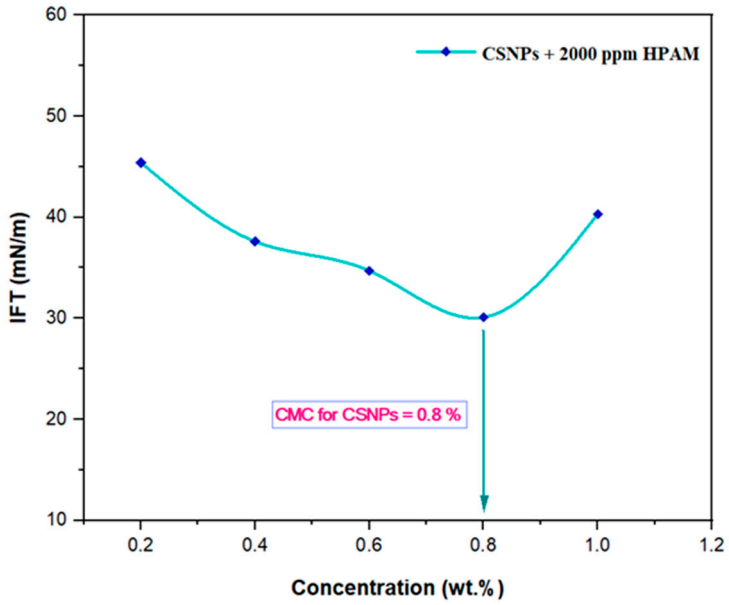

Figure 14. Relation between IFT and concentration for HPAM/CSNPs solution at 60 °C.

These values which represent CMC concentration for PYNPs and CSNP have been confirmed by measuring the viscosity of hybrid polymer solution for different concentrations of nanoparticles (0.2 to 1 wt.%) for period of 10 days. As shown in Figures 15, the viscosity of PYNPs is approximately stable during this period when the concentration of PYNPs is 0.6 wt.% except at the first day which its value is somehow higher than others. Also from Figure 16, the viscosity of CSNPs did not change much when the concentration of CSNPs is 0.8 wt.%. This gives more confirmation about the CMC values obtained before from IFT measurements. Therefore, these values are considered as the optimum concentration for the two kinds of nanoparticles in the polymer solution.

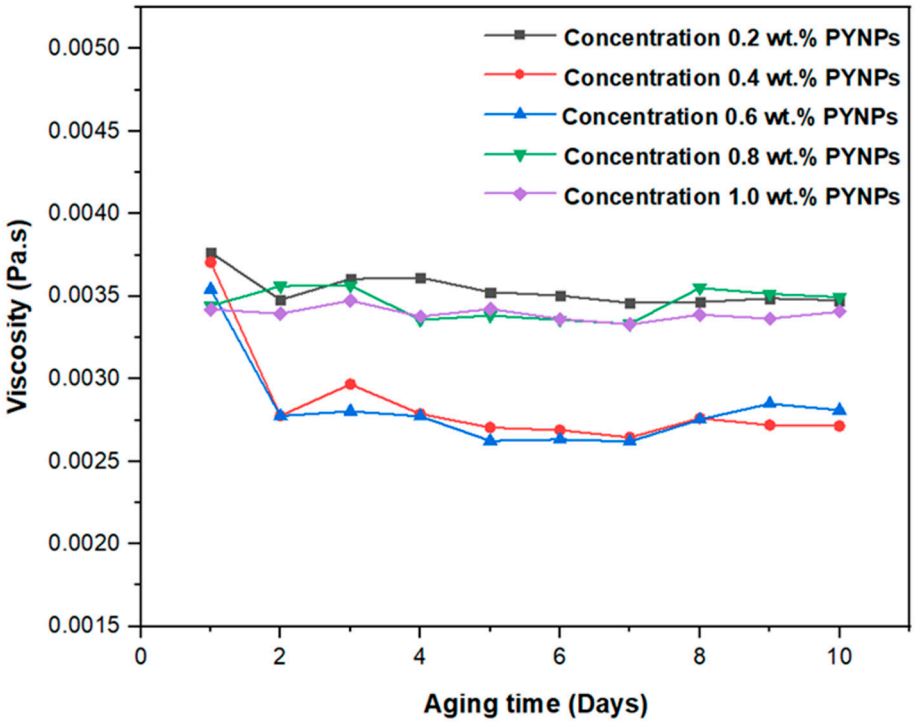

Figure 15. Relation between the viscosity of HPAM/PYNPs solution and the aging time (in days) for five concentrations of PYNPs.

Preprints (www.preprints.org) | NOT PEER-REVIEWED | Posted: 6 March 2023 doi:10.20944/preprints202303.0087.v1

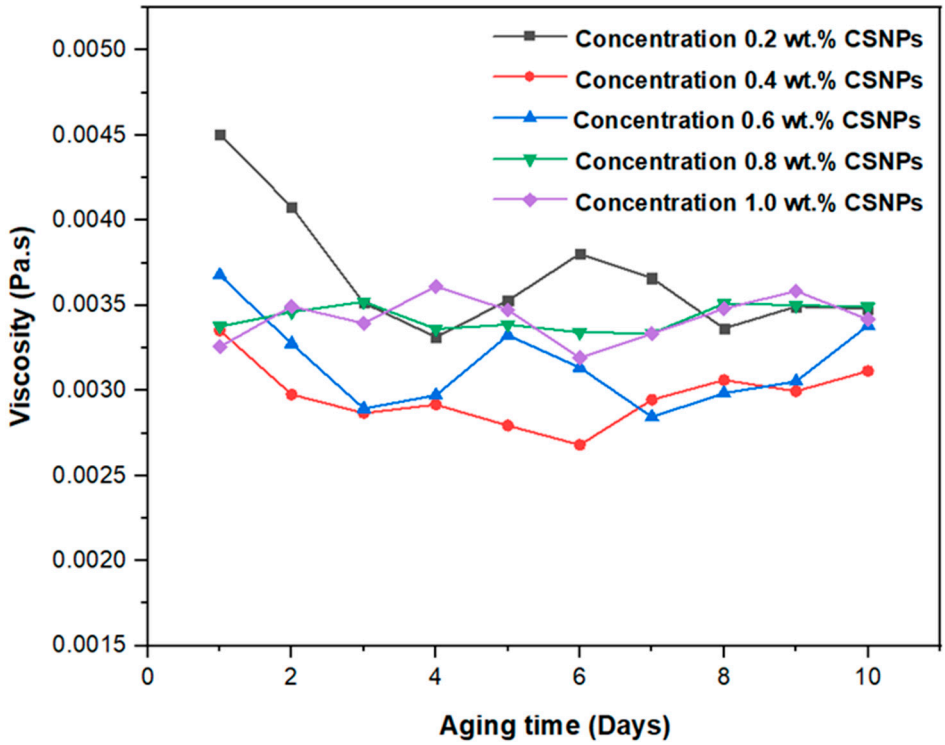

Figure 16. Relation between the viscosity of HPAM/CSNPs solution and the aging time (in days) for five concentrations of CSNPs.

3.7. Oil Recovery from Water and Polymer Flooding

Since Windsor type I is achieved for the combination of output liquid from polymer flooding with CSNPs as shown in Figure 17, therefore, water flooding or water plus polymer flooding using CSNPs/HPAM is not efficient enough in extracting large amount of oil from the core sample in comparison to water and polymer flooding with the solution consisted of PYNPs/HPAM solution as illustrated in Table 5.

Table 5. Oil recovery results from water and polymer flooding at 60 °C.

Flooding 1	RF%	Flooding 2	RF%
water flooding [1]	45	water flooding [2]	42.61
polymer flooding using HPAM/PYNPs	33.46	polymer flooding using HPAM/CSNPs	31.3
overall recovery (water + polymer) flooding	78.46	overall recovery (water + polymer) flooding	73.91

[1] Before implementing polymer flooding with HPAM/PYNPs. [2] Before implementing polymer flooding with HPAM/CSNPs.

Preprints (www.preprints.org) | NOT PEER-REVIEWED | Posted: 6 March 2023 doi:10.20944/preprints202303.0087.v1

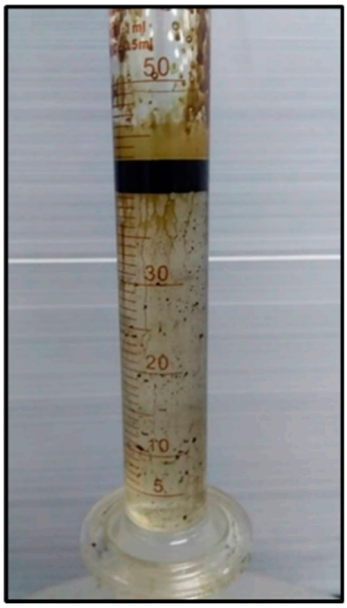

Figure 17. Oil extracted after water and polymer flooding at 60 °C. The polymer solution is consisted from 2000 ppm HPAM and 0.8 wt.% CSNPs.

It is clear as number indicates that polymer flooding with HPAM and PYNPs gave the best results in oil recovery in comparison to the other polymer combination. Despite the fact that there is no much difference between the two but the combination that contains PYNPs is more stable as Windsor type 3 has achieved as seen in Figure 18. Therefore, this technology has improved the conventional polymer flooding with HPAM through seeding 0.6 wt.% PYNPs in the solution. The relations between oil recovery and pore volume and that of oil recovery with time of injection for both kinds flooding are shown in Figures 19–22.

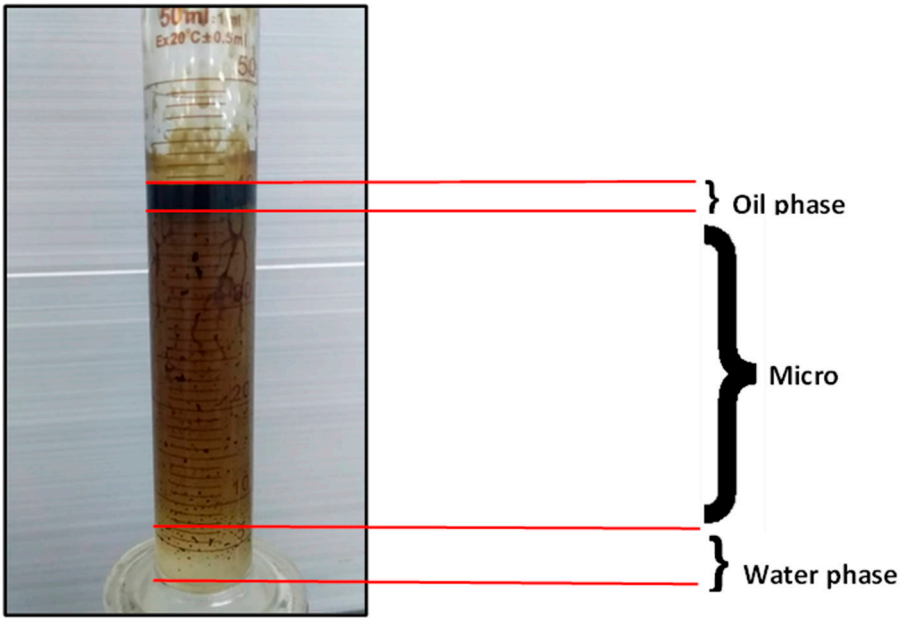

Figure 18. Oil extracted after water and polymer flooding at 60 °C. The polymer solution is consisted from 2000 ppm HPAM and 0.6 wt. % PYNPs.

Preprints (www.preprints.org) | NOT PEER-REVIEWED | Posted: 6 March 2023 doi:10.20944/preprints202303.0087.v1

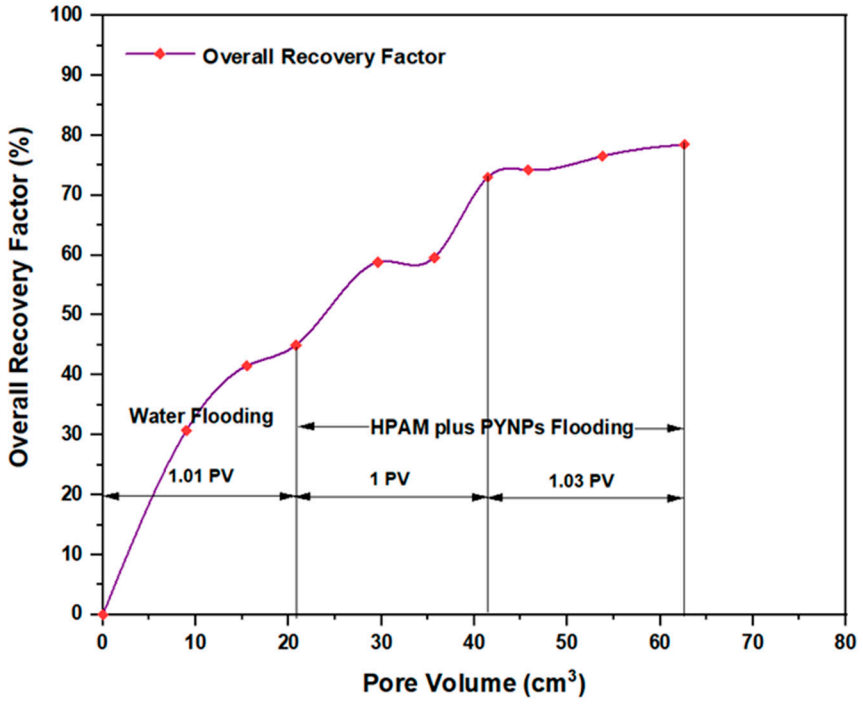

Figure 19. Overall oil recovery versus pore volume from water and polymer flooding at 60 °C. The polymer solution is consisted from 2000 ppm HPAM and 0.60 wt.% PYNPs.

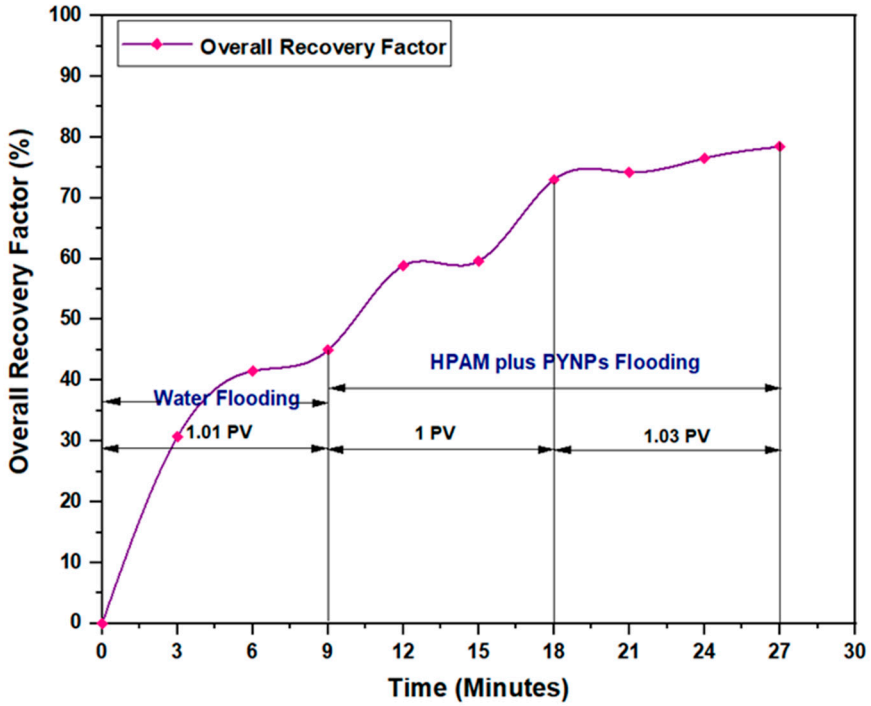

Figure 20. Overall oil recovery versus time of injection from water and polymer flooding at 60 °C. The polymer solution is consisted from 2000 ppm HPAM and 0.60 wt.% PYNPs.

Preprints (www.preprints.org) | NOT PEER-REVIEWED | Posted: 6 March 2023 doi:10.20944/preprints202303.0087.v1

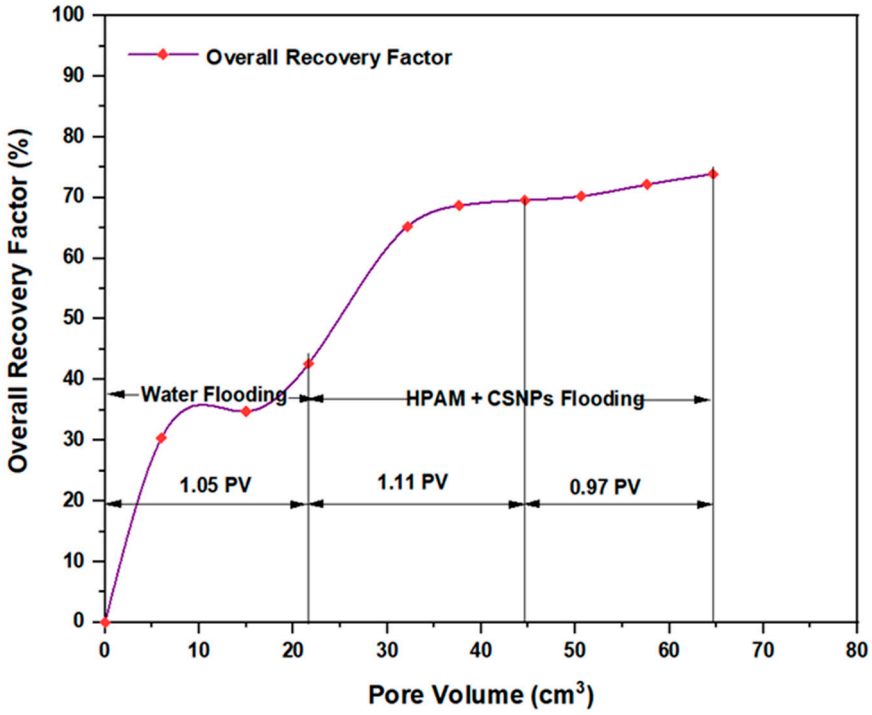

Figure 21. Overall oil recovery versus pore volume from water and polymer flooding at 60 °C. The polymer solution is consisted from 2000 ppm HPAM and 0.80 wt.% CSNPs.

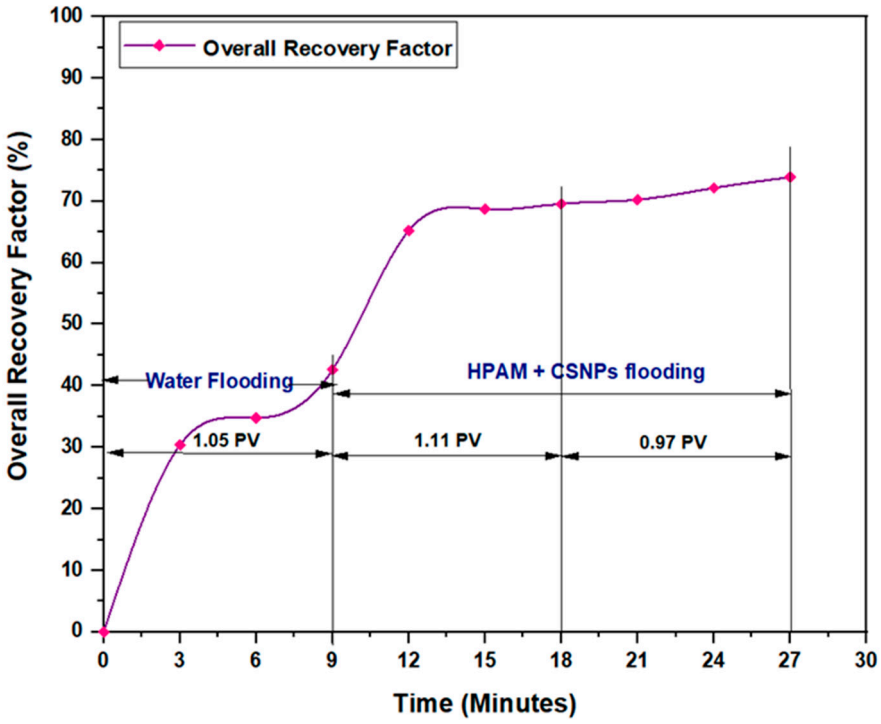

Figure 22. Overall oil recovery versus time of injection from water and polymer flooding at 60 °C. The polymer solution is consisted from 2000 ppm HPAM and 0.80 wt.% CSNPs.

The first relation gives the overall oil recovery versus quantity of solution injected and this quantity is expressed relative to the core pore volume. The second relation is between overall oil recovery against the time of injection. As seen from these figures, the first region is recognized for water flooding as water is first injected to the core sample. It was found that the quantity of water

Preprints (www.preprints.org) | NOT PEER-REVIEWED | Posted: 6 March 2023 doi:10.20944/preprints202303.0087.v1

injected is not exactly 1 PV, it was 1.01 PV for flooding 1 and 1.05 for flooding 2. The reason for this difference is related to the time of injection or more accurately the last two to three minutes of injection [48]. As the injection process is controlled to stop at the pre-set time (each 3 minutes) it happens that within last 2-3 minutes of flooding, 1 PV of solution has already been injected. Therefore, completing the cycle of operation resulted in excess injection for solution (water) into the core sample. The same thing occurred for the quantity injected by polymer flooding with nanoparticles and it was 2.03 PV for HPAM/PYNPs and 2.08 PV for HPAM/CSNPs solution.

4. Conclusions

In this study new natural materials have been involved in polymer flooding to improve the recovery of oil in comparison to the conventional polymer flooding that employ HPAM. These natural materials are obtained from purple yam and cassava starches and the process involved decreasing their particle sizes to nano scale to improve their properties. Based on the experimental results, it was possible to synthesis large quantity of nanoparticles and this has been confirmed from TEM images. The average particle size for PYNPs is 363.12 nm and that for CSNPs is 52.92 nm based on intensity percent measurements.

According to zeta potential distribution, PYNPs are more stable in comparison to CSNPs as mean zeta potential was -36.3 mv for PYNPs and -10.7 mv for CSNPs. The yield of produced PYNPs was somehow smaller than CSNPs (85% for PYNPs and 90.53% for CSNPs). From IFT and polymer rheology measurements it was confirmed that the optimum concentration for PYNPs is 0.60 wt.% and that for CSNPs is 0.80 wt.%. For DSC analysis, the melting point for these nanoparticles was 97.6 ^{o}C for PYNPs and 97.8 ^{o}C for CSNPs, therefore, both of them is considered satisfactory when applied in polymer flooding into a reservoir under temperature of 60 ^{o}C like Langgak oilfield.

It can conclude that produced nano-polymers from both two kinds have improved oil recovery through involving them in polymer flooding with HPAM after water flooding. On anyway, the oil recovered from PYNPs solution was higher than that obtained from CSNPs (33.46% for PYNPs and 31.3% for CSNPs). This is confirmed from phase equilibria as Windsor type III is achieved through using HPAM/PYNPs solution as shown in Figure 18. Accordingly, Windsor type I has obtained from polymer flooding with HPAM/CSNPs combination as shown in Figure 17. Windsor type III is more preferable in oil industry and it refers to an efficient oil recovery [49]. Thus, overall oil recovery based on PYNPs has raised to 78.46% and that for the other nano polymer 73.91% whereas polymer flooding with HPAM alone has led to an overall oil recovery of 50% according to a study performed by Rellegadla et al. [10].

Author Contributions: Writing - Original Draft Preparation, Hasanain A. AL-Jaber; Supervision, Agus Arsad and Sulalit Bandyopadhyay; Data curation, Agus Arsad; Project Administration, Muhammad Tahir; Conceptualization, Mustafa Jawad Nuhma; Validation, Abdulmunem R. Abdulmunem and Anis Farhana Abdul Rahman; Information and Data Collection, Abdulmunem R. Abdulmunem; Resources, Zakiah binti Harun; Writing - Review & Editing, Agi Augustine.

Funding: The authors would like to express their high appreciation for the financial support received from School of Chemical and Energy Engineering, Universiti Teknologi Malaysia (UTM) through the Grant No. R.J130000.7351.4B549 and Q.J130000.3551.07G11.

Acknowledgments: The authors express their higher appreciation to the staff of Reservoir Laboratory especially Mr. Roslan Jas for dedicating time to elaborate on using equipments and for providing some materials for the experimental work.

Conflicts of Interest: The authors declare that there is no conflict of interest throughout the period of this study.

Preprints (www.preprints.org) | NOT PEER-REVIEWED | Posted: 6 March 2023 doi:10.20944/preprints202303.0087.v1

Nomenclature

EOR	Enhanced oil recovery
FTIR	Fourier transform infrared spectroscopy
DSC	Differential scanning calorimetry
NPs	Nanoparticles
OOIP	Original oil in place
HPAM	Partially hydrolyzed polyacrylamide
PYNPs	Purple yam nanoparticles
CSNPs	Crystalline starch Nanoparticles
DMRT	Duncan's multiple range test
RSM	Response surface methodology
SEM	Scanning electron microscopy
TEM	Transmission electron microscopy
PSA	Particle size distribution
PDI	Polydispersity index
PYS	Purple yam starch
CAS	Cassava starch
CASPAM	Cassava starch-grafted-polyacrylamide
CMC	Critical micelle concentration
CMSP	Cationic modified starch polymer
IFT	Interfacial tension (mN/m)
PV	Pore volume of sandstone core (cm^3)
RF	Recovery factor for oil (%)
ppm	Part per million
WCSNP	Final weight of produced nanoparticles (g)
WNS	Initial weight of native starch (g)
Vw	Volume of water produced during oil injection (cm^3) ≈ OOIP

References

1. Cheraghian, G., & Hendraningrat, L. (2016). A review on applications of nanotechnology in the enhanced oil recovery part B: effects of nanoparticles on flooding. *International Nano Letters*, *6*(1), 1–10. https://doi.org/10.1007/S40089-015-0170-7.
2. Azizi Samir, M. A. S., Alloin, F., & Dufresne, A. (2005). Review of Recent Research into Cellulosic Whiskers, Their Properties and Their Application in Nanocomposite Field. *Biomacromolecules*, *6*(2), 612–626. https://doi.org/10.1021/BM0493685.
3. Viswanathan, V., Laha, T., Balani, K., Agarwal, A., & Seal, S. (2006). Challenges and advances in nanocomposite processing techniques. *Materials Science and Engineering: R: Reports*, *54*(5–6), 121–285. https://doi.org/10.1016/J.MSER.2006.11.002.
4. Scientific Research Publishing (n.d.). Hubbe, M.A., Rojas, O.J., Lucia, L.A. and Sain, M. (2008). Cellulosic Nanocomposites A Review. *BioResources*, *3*, 929-980. Available online: https://www.scirp.org/%28S%28czeh2tfqyw2orz553k1w0r45%29%29/reference/referencespapers.aspx?referenceid=2483299 (accessed on 26 June 2022).
5. Neethirajan, S., & Jayas, D. S. (2011). Nanotechnology for the food and bioprocessing industry. *Food and Bioprocess Technology*, *4*, 39-47. https://doi.org/10.1007/s11947-010-0328-2.
6. Van Mele, B., Van Assche, G., & Van Hemelrijck, A. (2016). Modulated Differential Scanning Calorimetry to Study Reacting Polymer Systems. *Journal of Reinforced Plastics and Composites*, *18*(10), 885-894. https://doi.org/10.1177/073168449901801002.
7. Dufresne, A. (2008). Polysaccharide nanocrystal reinforced nanocomposites. *Canadian Journal of Chemistry*, *86*(6), 484-494. https://doi.org/10.1139/v07-152.
8. Pérez, S., & Bertoft, E. (2010). The molecular structures of starch components and their contribution to the architecture of starch granules: A comprehensive review. *Starch-Stärke*, *62*(8), 389-420. https://doi.org/10.1002/star.201000013.

Preprints (www.preprints.org) | NOT PEER-REVIEWED | Posted: 6 March 2023 doi:10.20944/preprints202303.0087.v1

9. Visakh, P. M., & Thomas, S. (2010). Preparation of bionanomaterials and their polymer nanocomposites from waste and biomass. *Waste and Biomass Valorization, 1*(1), 121-134. https://doi.org/10.1007/S12649-010-9009-7.
10. Rellegadla, S., Prajapat, G., & Agrawal, A. (2017). Polymers for enhanced oil recovery: fundamentals and selection criteria. *Applied Microbiology and Biotechnology*, *101*(11), 4387–4402. https://doi.org/10.1007/S00253-017-8307-4/FIGURES/5.
11. Ahmad, N., Sharma, S., Alam, M. K., Singh, V. N., Shamsi, S. F., Mehta, B. R., & Fatma, A. (2010). Rapid synthesis of silver nanoparticles using dried medicinal plant of basil. *Colloids and Surfaces B: Biointerfaces, 81*(1), 81-86. https://doi.org/10.1016/j.colsurfb.2010.06.029.
12. Saeng-on, J., & Aht-Ong, D. (2017). Production of starch nanocrystals from agricultural materials using mild acid hydrolysis method: Optimization and characterization. *Polymers from Renewable Resources*, *8*(3), 91–116. https://doi.org/10.1177/204124791700800302.
13. Skauge, T., K. Spildo, and A. Skauge. (2010). Nano-sized particles for EOR. Proceedings –*SPE Symposium on Improved Oil Recovery* 2: 1281–90. https://doi.org/10.2118/129933-ms.
14. Cheraghian, G., S. S. Khalili Nezhad, M. Kamari, M. Hemmati, M. Masihi, and S. Bazgir. 2014. Adsorption polymer on reservoir rock and role of the nanoparticles, clay and SiO_2. *International Nano Letters, 4*(3):1–8. https://doi.org/10.1007/s40089-014-0114-7.
15. Nadia, L. (2014). Characterization of Physicochemical and Functional Properties of Starch from Five Yam (Dioscorea Alata) Cultivars in Indonesia. *International Journal of Chemical Engineering and Applications*, *5*(6), 489–496. https://doi.org/10.7763/IJCEA.2014.V5.434.
16. Matovanni, M. P. N., Distantina, S., & Kaavessina, M. (2022). Synthesis of Cassava Starch-Grafted Polyacrylamide Hydrogel by Microwave-Assisted Method for Polymer Flooding. *Indonesian Journal of Chemistry*, *22*(3), 791–804. https://doi.org/10.22146/IJC.71343.
17. Agi, A., Junin, R., Gbadamosi, A., Abbas, A., Azli, N. B., & Oseh, J. (2019). Influence of nanoprecipitation on crystalline starch nanoparticle formed by ultrasonic assisted weak-acid hydrolysis of cassava starch and the rheology of their solutions. *Chemical Engineering and Processing - Process Intensification*, *142*, 107556. https://doi.org/10.1016/j.cep.2019.107556.
18. Agi, A., Junin, R., Abdullah, M. O., Jaafar, M. Z., Arsad, A., Wan Sulaiman, W. R., Norddin, M. N. A. M., Abdurrahman, M., Abbas, A., Gbadamosi, A., & Azli, N. B. (2020). Application of polymeric nanofluid in enhancing oil recovery at reservoir condition. *Journal of Petroleum Science and Engineering*, *194*, 107476. https://doi.org/10.1016/J.PETROL.2020.107476.
19. Angellier, H., Choisnard, L., Molina-Boisseau, S., Ozil, P. and Dufresne, A. (2004) 'Optimization of the preparation of aqueous suspensions of waxy maize starch nanocrystals using a response surface methodology', *Biomacromolecules*, *5*(4), pp. 1545–1551. https://doi.org/10.1021/bm049914u.
20. Md Shahrodin, N. S., Rahmat, A. R. and Arsad, A. (2015) 'Synthesis and Characterization of Cassava Starch Nanocrystals by Hydrolysis Method', *Advanced Materials Research*, 1113, pp. 446–452. https://doi.org/10.4028/www.scientific.net/AMR.1113.446.
21. Mahbubul, I. M., Chong, T. H., Khaleduzzaman, S. S., Shahrul, I. M., Saidur, R., Long, B. D., & Amalina, M. A. (2014). Effect of ultrasonication duration on colloidal structure and viscosity of alumina-water nanofluid. *Industrial and Engineering Chemistry Research*, *53*(16), 6677–6684. https://doi.org/10.1021/IE500705J.
22. Müller, R. H., Rühl, D., & Runge, S. A. (1996). Biodegradation of solid lipid nanoparticles as a function of lipase incubation time. *International Journal of Pharmaceutics*, *144*(1), 115–121. https://doi.org/10.1016/S0378-5173(96)04731-X.
23. Hanaor D, Michelazzi M, Leonelli C, Sorrell CC (2012). The effects of carboxylic acids on the aqueous dispersion and electrophoretic deposition of ZrO_2. *Journal of the European Ceramic Society*, *32*(1), 235–244. https://doi.org/10.1016/j.jeurceramsoc.2011.08.015.
24. Suslick, K. S., Didenko, Y., Fang, M. M., Hyeon, T., Kolbeck, K. J., McNamara, W. B. (1999). Acoustic cavitation and its chemical consequences. *Philosophical Transactions of the Royal Society A, 357*, 335e353. https://doi.org/10.1098/rsta.1999.0330.
25. Lake, L. W. *Enhanced oil recovery*, 3rd ed.; Prentice Hall: Englewood Cliffs, NJ, 1989; pp. 247-256.
26. Eseimokumoh, I. B., Woyintonye, I., Eniye, O., Preye, T.-A. N., & Young, E. E. (2021). Improving Oil Recovery Efficiency Using Corn starch as a Local Polymer for Enhanced Oil Recovery Processes. *International Journal of Current Science Research and Review*, *04*(11). https://doi.org/10.47191/ijcsrr/V4-i11-07.

Preprints (www.preprints.org) | NOT PEER-REVIEWED | Posted: 6 March 2023 doi:10.20944/preprints202303.0087.v1

27. Barbucci, R., Pasqui, D., Favaloro, R., & Panariello, G. (2008). A thixotropic hydrogel from chemically cross-linked guar gum: synthesis, characterization and rheological behaviour. *Carbohydrate Research, 343*(18), 3058–3065. https://doi.org/10.1016/J.CARRES.2008.08.029.
28. He, F., & Zhao, D. (2005). Preparation and characterization of a new class of starch-stabilized bimetallic nanoparticles for degradation of chlorinated hydrocarbons in water. *Environmental science & technology, 39*(9), 3314-3320. https://doi.org/10.1021/es048743y.
29. Rodrigues, A., & Emeje, M. (2012). Recent applications of starch derivatives in nanodrug delivery. *Carbohydrate Polymers, 87*(2), 987-994. https://doi.org/10.1016/j.carbpol.2011.09.044.
30. Ku, B. K., & Maynard, A. D. (2006). Generation and investigation of airborne silver nanoparticles with specific size and morphology by homogeneous nucleation, coagulation and sintering. *Journal of Aerosol Science*, *37*(4), 452–470. https://doi.org/10.1016/J.JAEROSCI.2005.05.003.
31. Campelo, P. H., Sant'Ana, A. S., & Pedrosa Silva Clerici, M. T. (2020). Starch nanoparticles: production methods, structure, and properties for food applications. *Current Opinion in Food Science*, *33*, 136–140. https://doi.org/10.1016/j.cofs.2020.04.007.
32. Angellier, H., Molina-Boisseau, S., Lebrun, L., & Dufresne, A. (2005). Processing and structural properties of waxy maize starch nanoparticles reinforced natural rubber. *Macromolecules, 38*(9), 3783-3792. https://doi.org/10.1021/ma050054z.
33. Kessler, R. (2011). Engineered nanoparticles in consumer products: understanding a new ingredient. *Environmental health perspectives*, *Vol. 119*, Issue 3. https://doi.org/10.1289/ehp.119-a120.
34. Kaur, M., Oberoi, D. P. S., Sogi, D. S., & Gill, B. S. (2011). Physicochemical, morphological and pasting properties of acid treated starches from different botanical sources. *Journal of Food Science and Technology*, *48*(4), 460. https://doi.org/10.1007/S13197-010-0126-X.
35. Kaplan, D. L. (1998). Introduction to biopolymers from renewable resources. *Biopolymers from renewable resources* (pp. 1-29). Springer, Berlin, Heidelberg.
36. Kim, H. Y., Lee, J. H., Kim, J. Y., Lim, W. J., & Lim, S. T. (2012). Characterization of nanoparticles prepared by acid hydrolysis of various starches. *Starch-Stärke, 64*(5), 367-373. https://doi.org/10.1002/star.201100105.
37. Le Corre, D., Bras, J., & Dufresne, A. (2010). Starch nanoparticles: a review. *Biomacromolecules, 11*(5), 1139-1153. https://doi.org/10.1021/bm901428y.
38. Le Corre, D., &Angellier-Coussy, H. (2014). Preparation and application of starch nanoparticles for nanocomposites: A review. *Reactive and Functional Polymers, 85*, 97-120. https://doi.org/10.1016/j.reactfunctpolym.2014.09.020.
39. Madras, G., Kumar umar, S., & Chattopadhyay, S. (2000). Continuous distribution kinetics for ultrasonic degradation of polymers. *Polymer Degradation and Stability, 69*, 73-78. https://doi.org/10.1016/S0141-3910(00)00042-2.
40. Lu, D. R., Xiao, C. M., & Xu, S. J. (2009). Starch-based completely biodegradable polymer materials. *Express polymer letters, 3*(6), 366-375. https://doi.org/10.3144/expresspolymlett.2009.46.
41. Ma, X., Jian, R., Chang, P. R., & Yu, J. (2008). Fabrication and characterization of citric acid-modified starch nanoparticles/plasticized-starch composites. *Biomacromolecules, 9*(11), 3314-3320. https://doi.org/10.1021/bm800987c.
42. Song, D., Thio, Y. S., & Deng, Y. (2011). Starch nanoparticle formation via reactive extrusion and related mechanism study. *Carbohydrate Polymers*, 85, 208-214. https://doi.org/10.1016/j.carbpol.2011.02.016.
43. Simi, C. K., & Abraham, T. E. (2007). Hydrophobic grafted and cross-linked starch nanoparticles for drug delivery. *Bioprocess and biosystems engineering, 30*(3), 173-180. https://doi.org/10.1007/s00449-007-0112-5.
44. Tester, R. F., Karkalas, J., & Qi, X. (2004). Starch—composition, fine structure and architecture. *Journal of Cereal Science, 39*(2), 151-165. https://doi.org/10.1016/j.jcs.2003.12.001.
45. Yucel, T., Cebe, P., & Kaplan, D. L. (2009). Vortex-Induced Injectable Silk Fibroin Hydrogels. *Biophysical Journal*, *97*(7), 2044–2050. https://doi.org/10.1016/J.BPJ.2009.07.028.
46. Van der Werff, J. C., de Kruif, C. G., & Dhont, J. K. G. (1989). The shear-thinning behaviour of colloidal dispersions: II. Experiments. *Physica A: Statistical Mechanics and Its Applications*, *160*(2), 205–212. https://doi.org/10.1016/0378-4371(89)90417-2.
47. Price, G. J., & Smith, P. F. (1993). Ultrasonic degradation of polymer solutions. III. The effect of changing solvent and solution concentration. *European Polymer Journal, 29*, 419-424. https://doi.org/10.1016/0014-3057(93)90114-U.

Preprints (www.preprints.org) | NOT PEER-REVIEWED | Posted: 6 March 2023 doi:10.20944/preprints202303.0087.v1

48. Yang, S., Dai, C., Wu, X., Liu, Y., Li, Y., Wu, Y., & Sun, Y. (2017). Novel investigation based on cationic modified starch with residual anionic polymer for enhanced oil recovery. *Journal of Dispersion Science and Technology*, *38*(2), 199–205. https://doi.org/10.1080/01932691.2016.1154863.
49. Elraies, K. A. (2012). An experimental study on ASP process using a new polymeric surfactant. *Journal of Petroleum Exploration and Production Technology*, *2*(4), 223–227. https://doi.org/10.1007/s13202-012-0039-5.

Disclaimer/Publisher's Note: The statements, opinions and data contained in all publications are solely those of the individual author(s) and contributor(s) and not of MDPI and/or the editor(s). MDPI and/or the editor(s) disclaim responsibility for any injury to people or property resulting from any ideas, methods, instructions or products referred to in the content.